Eligiusz PAWŁOWSKI

Lublin University of Technology, Faculty of Electrical Engineering and Computer Science, Department of Automatics and Metrology

doi:10.15199/48.2016.07.07

Galvanic isolation circuit for measuring systems operating in environments with strong electromagnetic disturbances

***Abstract**. Measuring systems operating in environments with strong electromagnetic disturbances require proper technical solutions preventing excessive errors and measurement uncertainties. Commonly used solutions include shielding, earthing and galvanic isolation. This work presents a proposal for a new galvanic isolation circuit using a Light-to-Frequency Converter (LFC) working alongside a LED.*

***Streszczenie.** Systemy pomiarowe pracujące w środowisku silnych zakłóceń elektromagnetycznych wymagają stosowania odpowiednich rozwiązań zapobiegających pojawianiu się nadmiernych błędów pomiarowych. Stosuje się w tym celu ekranowanie, uziemianie oraz separację galwaniczną. W pracy przedstawia się propozycję nowego układu izolacji galwanicznej wykorzystującego przetwornik światło-częstotliwość sprzęgnięty z diodą LED. (**Układ separacji galwanicznej dla systemów pomiarowych pracujących w środowisku silnych zakłóceń elektromagnetycznych**).*

Keywords: galvanic isolation circuit, Light-to-Frequency Converter, LFC, electromagnetic disturbances.
Słowa kluczowe: układ izolacji galwanicznej, przetwornik światło-częstotliwość, zaburzenia elektromagnetyczne.

Introduction

Modern measuring systems often have to work in environments with strong electromagnetic disturbance. The result of this are additional measurement errors, increased risk of damage to devices and risk of equipment damage and danger of electric shock to human personnel [1]. There are a few ways, in which interferences may occur in measuring systems: direct galvanic connection, capacitive coupling, magnetic coupling and electromagnetic radiation. In order to reduce such effects, proper shielding, earthing and galvanic isolation are used [2]. Usage of galvanic isolation breaks the loop of common ground connecting each point of the measuring system with different potentials [3]. Therefore, we have some beneficial effects: currents flowing in the common ground wires, which are the source of interference, are terminated; common mode voltage and the risk of electric shock are reduced [1]. Figure 1 represents a simplified block diagram of a measuring system containing: sensor S, signal conditioning systems SCS, acquisition systems ADC, digital processing DSP and display D. Galvanic isolation GI marked with a dotted line may be introduced in many points of a measuring system, between ground points GND with different potentials. Due to measuring errors, the most beneficial mode of conduct is using galvanic isolation near the sensor S, where the signal is the weakest and the interference is the strongest [4].

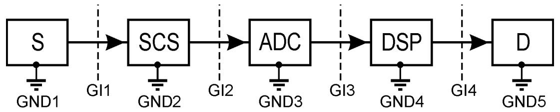

Fig.1. Simplified block diagram of a measuring system

Light-to-Frequency Converter

Modern galvanic isolation circuits use magnetic fields [1], electrical fields and light [5, 6] to transmit signals through the isolation barrier [2]. Galvanic isolation for analogue signal (GI1 and GI2 on fig. 1) requires a linear optocoupler. Commonly used optocouplers contain a LED optically coupled with two photodiodes [5, 6], which enable negative feedback, increasing the system's linearity. Many independent manufacturers offer such optocouplers [2].

Currently, there are also Light-to-Frequency Converters (LFC) [7], which enable a new type of galvanic isolation circuits. Using frequency as an information-carrying signal in the measuring system is very beneficial [8]. Frequency, in comparison with the voltage, is much more resistant to interference, can be sent over large distances without losing information and can be precisely converted into a digital form using cheap counters [9] or microcontrollers, without using expensive ADC converters [10].

LFC is an integrated circuit containing a photodiode connected to a current-to-frequency converter. A simplified electric diagram of such converter is presented on figure 2. However, real diagram is more complicated [11].

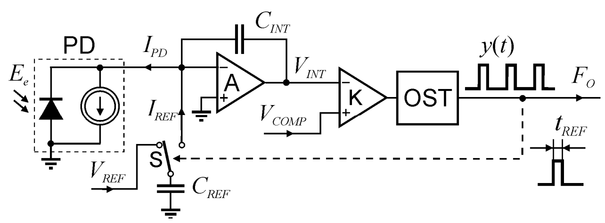

Fig.2. Simplified electric diagram of Light-to-Frequency Converter

Photodiode PD converts the incident irradiance E_e to current I_{PD} with the sensitivity of the photodiode S_{PD}. Integrator containing amplifier A and capacitor C_{INT}, comparator K, one-shot trigger OST and reference capacitor C_{REF} create a current-to-frequency converter. The principle of working of the LFC at steady state (E_e=*const.*) is explained in a time courses of signals given in figure 3 [12].

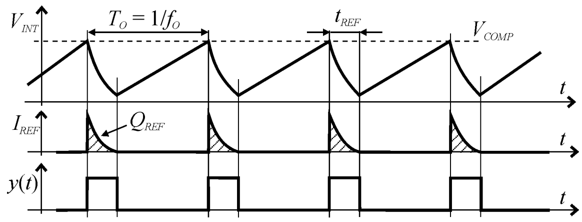

Fig.3. Time courses of signals in Light-to-Frequency Converter

Reference capacitor C_{REF} is periodically charged to the reference voltage V_{REF} and connected via switch S to the integrator input. The photodiode current I_{PD} is continuously integrated by integrator, so when the output voltage of the integrator V_{INT} reaches the comparator threshold voltage V_{COMP}, the one-shot trigger OST is triggered and a fixed time duration t_{REF} impulse on the converter output is generated. At the same time the capacitor C_{REF} is switched from the reference voltage V_{REF} to the summing node of the amplifier A. This way the LFC output signal $y(t)$ is a sequence of rectangular pulses. After time t_{REF} capacitor C_{REF} is switched back to the reference voltage V_{REF} to charging it for the next cycle. Negative feedback in this circuit causes the average current value I_{REF} supplied by the capacitor C_{REF} to the integrator to be equal to the photodiode's current value I_{PD}. This way the output frequency F_O is proportional to the incident irradiance E_e [7]:

$$(1)\qquad F_O = \frac{S_{PD}}{V_{REF}C_{REF}}E_e + F_D = R_e E_e + F_D ,$$

where: S_{PD} is the photodiode sensitivity given in A/(μW/cm^2), V_{REF} is the reference voltage given in V, C_{REF} is the reference capacitance given in F, E_e is the incident irradiance given in μW/cm^2, R_e is the LFC responsivity given in Hz/(μW/cm^2), F_D is the output frequency for dark condition (E_e=0) given in Hz. Such converters have a dynamic range of even 160 dB, nonlinearity of 0.1% of the measurement range and output frequency up to 1 MHz [7].

Proposed new galvanic isolation circuit

Using a LFC together with a LED enables a galvanic separation circuit for analogue signals. An appropriate block diagram is shown on figure 4. It works as follows: the LED converts the current I_F to radiant flux Φ_e, which uses the transmission medium TM to fall on the photodiode PD placed in the LFC. The photodiode current I_{PD} is continuously converted to the output frequency F_O by the current-to-frequency converter CFC in the same way described previously. The output frequency F_O is proportional to the current I_F flowing through the LED :

$$(2)\qquad F_O = \frac{CTR}{V_{REF}C_{REF}} I_F$$

where: CTR – current transfer ratio of the photodiode current I_{PD} to the LED current I_F:

$$(3)\qquad CTR = \frac{I_{PD}}{I_F} \ .$$

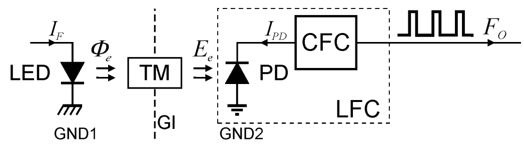

Fig.4. Block diagram of the galvanic isolation circuit

Static properties of the circuit

In order to assess metrological parameters of the proposed solution, a system was built in accordance with figure 4, using TSL235R TAOS Light-to-Frequency Converter [7] and IRL81A LED. Listed responsivity R_e of the LFC is 580 Hz·μW^{-1}cm^2 for 635 nm light wavelength, but maximum sensitivity occurs for 760 nm light wavelength [7]. In order to obtain nominal output frequency F_O=500 kHz, a incident irradiance E_e of 0,7 mW·cm^{-2} is required. The IRL81A diode generates a flux Φ_e with a radiant intensity of I_e=1 mW·sr^{-1} for current I_F=20 mA, by maximum radiation for 880 nm light wavelength. In order to obtain proper optical coupling (with medium value of CTR on fig. 5), both elements have been placed in the free air, 1 cm of each other, and enclosed in a lightproof case with black internal walls. Then, static processing characteristic of the system has been designated experimentally for three different CTR values, using a logarithmic scale on figure 5. The circuit operates correctly within about 120 dB, which corresponds to frequency values F_O of the LFC from 0,5 Hz to 800 kHz. Nonlinearity depends on the CTR, it is better for higher values of the CTR (line 1 on fig. 5).

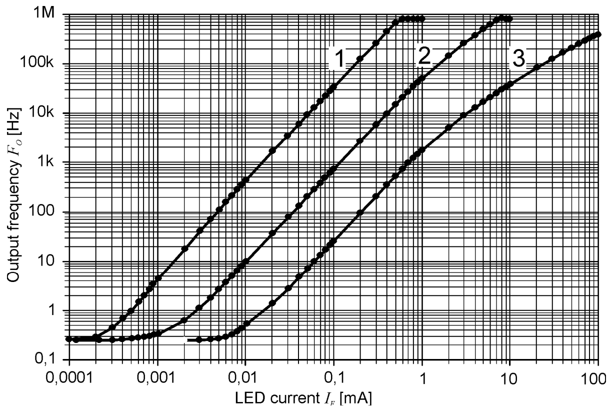

Fig.5. Static characteristic of the galvanic isolation circuit for different values of CTR: 1-high, 2-medium, 3-low

Circuit operation in dynamic conditions

In dynamic conditions, the LED current value I_F is changing, therefore output frequency F_O is also changing. In order to determine instantaneous values of input current I_F, it is necessary to measure instantaneous frequencies F_O. It requires usage of a system, which enables measuring all subsequent time intervals between subsequent output impulses of the converter [13]. In order to assess the operation of the system in dynamic conditions, a National Instruments NI 6602 measuring card connected to a PC has been used. Appropriate block diagram is shown in figure 6.

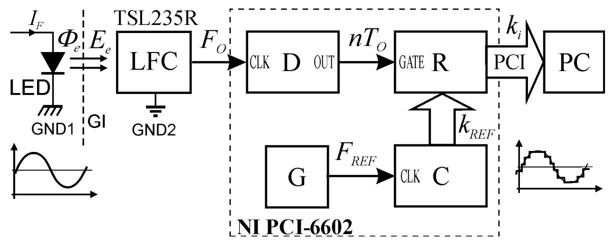

Fig.6. Block diagram of the measurement system

Two counters are used, the first of them works as frequency divisor D, the second one C is set in buffered period measurement mode [14] and counts reference frequency pulse F_{REF} from a generator G. The LFC output signal is fed to the divisor D. The output of the divisor is connected to the latch input GATE of the buffer register R, so at each rising edge of the pulse the current value k_i of the counter C is written to the register R and is sent via PCI bus to PC. A procedure of appropriate signal processing is shown in figure 7.

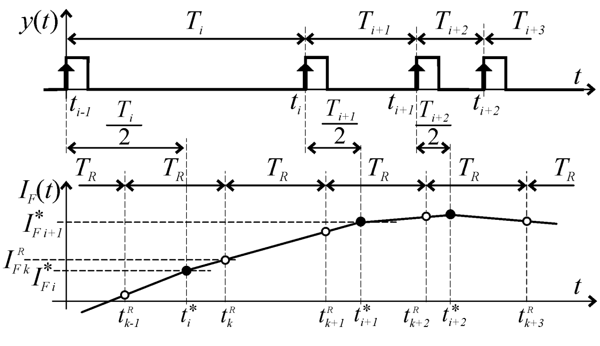

Fig.7. Linear interpolation of the frequency signal from LFC

Inter-pulse time values are given as T_i=t_i–t_{i-1}, where t_i=k_i/F_{REF}. Successive values of the LED current $I^*_{F\,i}$ can be determined as follow:

$$I^*_{F\,i} = \frac{V_{REF} C_{REF}}{CTR} \frac{1}{T_i} = \frac{V_{REF} C_{REF}}{CTR} \frac{F_{REF}}{k_i - k_{i-1}} . \quad (4)$$

The values of the current $I^*_{F\,i}$ are not instantaneous values, but they are average values for times T_i, which are obtained at moments t_i distributed nonuniformly in time. Assuming a linear change of the current I_F during time T_i, its average value $I^*_{F\,i}$ is equal to the instantaneous value $I_F(t)$ at moment t_i^*, lying in the middle of the time interval T_i [12]:

$$I^*_{F\,i} = I_F\left(t_i^*\right) , \; t_i^* = t_{i-1} + \frac{T_i}{2} . \quad (5)$$

Figure 8 shows results for harmonic input current with a constant value of 0,5 mA and an amplitude of 0,3 mA, changing with the frequency of 200 Hz. The graph also shows that for lower current values, the signal samples are spread less frequently, and for higher values – more frequently, therefore sampling is nonuniform, which makes it difficult to cooperate with voltage signals in the measuring system [10] and prevents the implementation of algorithms for the time and frequency analyses of signals [15].

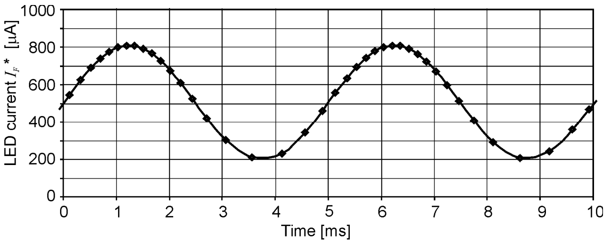

Fig.8. Sample measuring results in dynamic conditions with nonuniform sampling of frequency signal

In practice, it is more convenient to process the instantaneous values of signals sampled uniformly in time, which requires to perform a resampling by interpolating the current values $I_F(t)$ at intervals T_i between the measured values $I^*_{F\,i}$ and by collecting new values $I^R_{F\,k}$ at regular time intervals T_R=$const$ [16]. Successive points $I^*_{F\,i}$, t_i^* (5), shown in figure 7 (black dots), determine successive sections of a polyline interpolating current $I_F(t)$ at time intervals from $t_i^*=t_{i-1}+T_i/2$ to $t_{i+1}^*=t_i+T_{i+1}/2$, the polyline allowing for a uniform resampling by collecting current values $I^R_{F\,k}$ (white dots) at moments t^R_k equally spaced in time by a uniform sampling period T_R:

$$I^R_{F\,k} = I_F\left(t^R_k\right) = \frac{\left(t^R_k - t^*_i\right) I^*_{F\,i+1} + \left(t^*_{i+1} - t^R_k\right) I^*_{F\,i}}{t^*_{i+1} - t^*_i} \quad (6)$$

where: $t^R_k = kT_R$, $t^R_k \in \left(t^*_i , t^*_{i+1}\right)$.

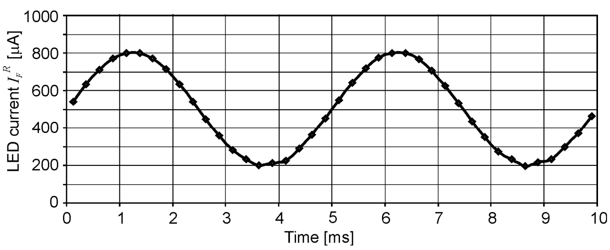

Fig.9. Samples of LED current I^R_F after uniform resampling

Example results for the uniform resampling (6) obtained from presented algorithm are shown in figure 9. Nonuniform sampling signal (fig. 8) was uniformly resampled with a period T_R=200μs. As can be seen, all samples are equally spaced in time by a uniform sampling period 200μs.

Summary

A new concept of a galvanic isolation system using a Light-to-Frequency Converter working alongside a LED is presented. Besides introducing the isolation barrier, using a frequency-measuring signal additionally increases resistance to strong electromagnetic interference. Results from a prepared system confirm proper linearity of static characteristic. After using an appropriate measuring system and an additional data processing algorithm, the circuit may also operate in dynamic conditions. In this case the instantaneous frequency may be determined easily as the inverse of the time between subsequent impulses and should be assigned to the moment in time present midway in this time. Therefore, received results are placed irregularly in time. In order to obtain signal samples placed regularly in time, an approximation of the converter's output signal may be used, and new samples at regular time intervals may be specified.

***Author**: dr inż. Eligiusz Pawłowski, Politechnika Lubelska, Wydział Elektrotechniki i Informatyki, ul. Nadbystrzycka 38A, 20-618 Lublin, e-mail: e.pawlowski@pollub.pl*

REFERENCES

[1] Zhang Z., Lee W., Dini D.A., Grounding and Isolation of Sensitive Measurement Equipment for Arc Flash Testing at High-Power Laboratory, *IEEE Transactions on Industry Applications* 51 (2015), no. 6, 5281-5287.

[2] Texas Instruments Inc., AN-298 Isolation Techniques for Signal Conditioning, *Application Report SNOA604B*, (2013).

[3] Lazar J., Jedlika P, Cip O., Ržika B., Laser diode current controller with a high level of protection against electromagnetic interference, *Review of Scientific Instruments* 74, (2003), no. 8, 3816-3819.

[4] Cięszczyk S., Sensors signal processing under influence of environmental disturbances, *Przegląd Elektrotechniczny* 89 (2013), nr 4, 129-131.

[5] Camin D. Pessina G., Differential optocoupler amplifier with low noise, low power and balanced output, *IEEE Transactions on Nuclear Science,* 47 (2000), no. 6, 2039-2044.

[6] Anjom M. K., Moslehi S., A novel approach to analog signal isolation through digital opto-coupler (YOUTAB), *Modern Applied Scienc* 5 (2011), no. 3, 225-230.

[7] TAOS, TSL235R Light-to-Frequency Converter, Texas Advanced Optoelectronic Solutions, *TAOS038E*, (2007).

[8] Pawlowski E., Resolution of a measurement chain with uniform sampling of the frequency signal, *Measurement Automation and Monitoring* 58 (2012), no. 11, 937-940.

[9] Pawlowski E., Digital processing of pulse signal from light-to-frequency converter under dynamic condition, *Proc. SPIE 9291* (2014), 929102/1-929102/6.

[10] Swisulski D., Methods of simultaneous acquisition in systems with voltage and frequency channels, *Przegląd Elektrotechniczny* 88 (2012), nr 10A, 29-31.

[11] Aswell, C. J., Berlien, J., Dierschke, E., Hassan, M., A monolithic light-to-frequency converter with a scalable sensor array, *SSC Int. Conf. Digest Tech. Papers* 41 (1994), 158-159.

[12] Pawlowski E., Simulation of sensor signal with frequency output, *Przegląd Elektrotechniczny* 88 (2012), nr 10B, 78-81.

[13] Warda P, Generator z modulacją częstotliwości jako źródło sygnału testującego dla toru pomiarowego z częstotliwościowym nośnikiem informacji, *Przegląd Elektrotechniczny*, 86 (2010), nr 8, 235-238.

[14] National Instruments, DAQ 6601/6602. High-speed counter/timer for PCI or PXI bus systems, *User Manual* (1999), 322137B-01.

[15] Hanus R., Estimating time delay of random signals using Hilbert Transform and analytic signal, *Przegląd Elektrotechniczny* 88 (2012), nr 10A, 46-48.

[16] Pawlowski E., Reconstruction of input signal of sensor with frequency output, *20th International Conference on Methods and Models in Automation and Robotics (MMAR),* IEEE, (2015), 909-914.